International Journal of Modern Manufacturing Technologies
ISSN 2067–3604, Vol. XIV, No. 2 / 2022
https://doi.org/ 10.54684/ijmmt.2022.14.2.286

MONITORING AND ANALYZING THE CLASSICAL COUNTER CURRENT INDUSTRIAL TUNNEL DRYER FOR MASONRY CLAY UNITS

Milos Vasić

"Institute for testing of materials", Bulevar vojvode Mišića 43 1100 Belgrade, Serbia

Corresponding author: Milos Vasic, milos.vasic@institutims.rs

Abstract: This paper goal was to increase the quality of the drying ware and to lower the drying scarp rate in one local brick factory. The registration of drying air parameters (temperature, humidity and velocity) along the dryer channels as well as the drying ware linear shrinkage and mass change were monitored for a month. Material and Energy balances were also recorded. Results have revealed that the drying air humidity and temperature profiles were not evenly distributed along the height of the drying tunnels. The ambient air breakthrough into the dryer was experimentally identified and quantified. It was the cause of the product quality deterioration and the reason why the critical and residual moisture in some of the products was larger than the desired one. Based on monitored data and mass and energy balances a solution was proposed for preventing the "false" air breakthrough, upgrade of the existing dryer fans and installation of the novel, measuring equipment. A hypothetical solution for increasing the capacity of the dryer, which uses the registered material and energy balances as well as factory management expectation, that the production of 50.000 masonry units per day will be achieved soon, was given also.
Key words: monitoring, industrial tunnel, dryer

1. INTRODUCTION

One of the EU's strategy and legislative objectives related with the more efficient use of energy and resources was naturally embedded into the actions plans for the enhancement production of clay brick and roofing tiles. Permanent and internal factory production control (FPC) has two purposes. The first one is to guarantee that the declared level of the masonry product essential characteristics are in accordance with the declaration of performance while the second one is to identify the critical production spots which needs to be upgrade, change or adapt. In such horizontal framework data gathered in FPC are input elements for making the decision of further product or process optimization [1-2]. H. Shoukouhmand has proposed a model for the more efficient chamber dryer design, in which the moving central fan has been replaced, by two axial recirculation fans, and two extra burners were added to reheat the circulating air. More uniform air velocity and temperature profiles in comparison to the classical chamber dryer design were experimentally confirmed. This model is also user friendly as its outputs are clearly specifying the desired values of the inlet air temperature and humidity, burner characteristic and axial fans optimal positions in the dryer [3]. Dolanc has presented a complex system in which the change of air flow rate as well as the outgoing waste air humidity fluctuations were correlated respectively with the relevant dumpers movement. This solution is widely accepted in the brick and roofing tile industry. Its efficiency has been numerously experimentally confirmed [4]. Velthuis and Dissen have developed the drying simulation software "DrySim" for optimization of chamber and tunnel dryers. The computation was based on the receding front theory, and requires that some of the input parameters which are not preset should be determined experimentally on a fully-scale green product in a special portable semi-laboratory dryer [5]. Telljoman, Junge and Specht have shown that the dependence of the moisture diffusion coefficient with the water volumetric fraction can be effectively used for foreseeing: the time dependent moisture and shrinkage profiles, drying curve, evaporation rate as well for computation of the air, product core and surface temperature change during drying. This model was experimentally confirmed and has been extensively used by German notified bodies during the FPC verification process as a tool used for fast comparison of the simulated and industrially documented drying curves [6]. Mancuhan has found a way to eliminate the condensation problem in the stack and in the tunnel dryer. The objective function which represents the total drying costs was firstly defined. It has included the costs of heating (released from hot air and taken by the outdoor air), costs to keep the stack temperature as lower as possible, costs of the heat required to evaporate the water from the products and the cost of electricity used to power the fans. The optimization of this function was the essence of the proposed method. The recommended stack temperature and relative humidity were defined as 47^{0}C and 80% respectively when the drying air was a mixture of the hot air at 200^{0}C and the outdoor air at 30^{0}C with relative humidity of 40% [7]. Vasić has shown that in the case of isothermal drying all mechanisms of moisture transport are visible on the time-dependent effective diffusivity curve. The segmented non-isothermal drying regime, in which different drying air parameters (temperature, relative humidity and velocity) as well as active moisture transport mechanisms were preset in accordance with the moisture transport theory within the first four isothermal segments, was than reported. Duration of these drying segments was equal to the time period in which the moisture transport mechanisms identified on the corresponding isothermal - time dependent effective diffusivity curve was active. This procedure was validated in the roofing tile factory. It was shown that the total drying time was decreased while the products have satisfied all quality requirements specified in EN 1304 [8-9].

2. CLASSICAL COUNTER-CURRENT TUNNEL DRYER - DETERMINATION OF THE CONSTANT ZONE LENGTH

This type of dryer is schematically presented on figure 1. It has two drying rate zones: the constant and the falling. Letters G, Fd, w, H and Tg are respectively representing the hot air mass flow rate (kg-dry air/s), the "processed" rate of dry ware (kg-dry solid/s), products moisture content (kg-water/kg-dry solid), the drying air humidity and temperature. The subscript 0 and 1 are assigned to the inlet and outlet of the dryer, while the subscript c and d are used to designate the end of the constant and the falling drying zone.

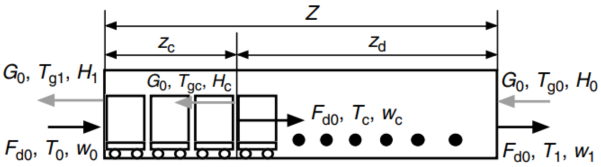

Fig. 1. Schematic view of the classical counter-current tunnel dryer

The mass conservation law for the constant drying zone is mathematically described via equation (1). Letters Rc, a, k_H, h and c_{gw} are respectively representing the value of the constant drying rate, the specific surface area of the green ware per unit length of the dryer, mass transfer coefficient, heat transfer coefficient and specific heat of wet air. Subscript s is describing that the air is in the saturated state. If Hs is assumed to be constant, and mass transfer coefficient is calculated from the Lewis simplified law, equation (3) is defining the theoretical length of the constant dryer zone.

$$F_{d0}(w_0 - w) = G_d(H_1 - H); \quad -F_{d0}dw = -G_d dH = R_c a dz \quad (1)$$

$$R_c = k_H(H_s - H) = \frac{h}{\lambda}(T_g - T_s); \quad k_H \approx \frac{h}{C_{gw}} \quad (2)$$

$$Z_c = \frac{G_0}{k_H a}\int_{H_c}^{H_1}\frac{dH}{H_s - H}; \quad Z_c = \frac{G_0 C_{gw}}{ha}\ln\frac{H_s - H_c}{H_s - H_1} \quad (3)$$

3. RESULTS AND DISCUSSION

The classical "Keller" counter current dryer presented at figure 2, was externally analyzed and monitored in April 2018. The Ahlborn THERM 3256-6 and TMI-ORION Cerydry data loggers with the corresponding sensors were used for registration of drying air temperature, humidity and linear shrinkage while the United Sensors Pitot-Static tubes type PCD-12-KL with kc of 1.0, digital pressure gauge of 20 mbar and anemometer with turbine were used for measuring the drying air velocity.

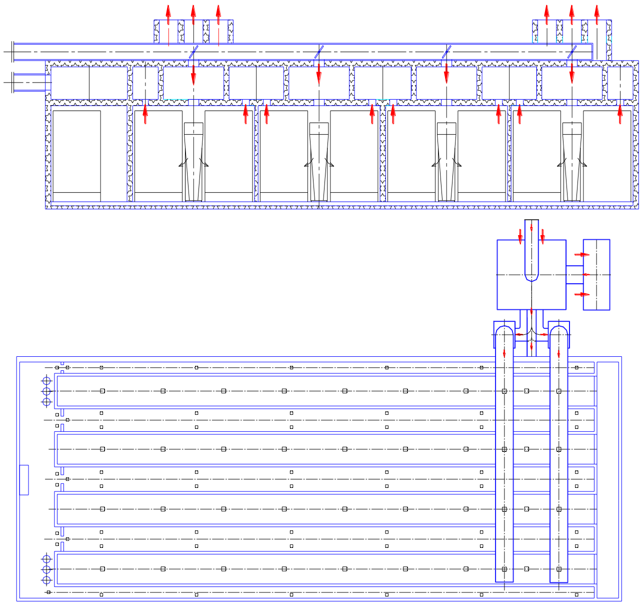

Fig. 2. Keller dryer

The analyzed dryer has four drying and one returning tunnel. Each channel is 61.6 m long and is equipped with two drying tracks and thirteen cornet air batteries. Six green hollow blocks with vertical voids (250x190x190 mm) are forming the first drying ware raw (DWR). Typical drying ware wagon (DWW) has 11 DWRs. Twenty seven DWW are forming a drying batch on each drying track. The maximal capacity of the dryer is 212 DWW. The hot air used for drying is a mixture of the "waste" air taken from the outlet kiln duct and the "fresh" air taken from the dryer heat generator. It is transported through the ceiling ducts to the corresponding drying tunnels. Installed cornet mixers were used to distribute the delivered hot air evenly throughout the drying tunnels.
The list of inlet and outlet measuring points as well as the identified "false" air breakthrough positions is

given in table 1. The temperature, air relative humidity and product shrinkage was registered at II, VI and X DWR, while the mass loss and the product temperature were recorded in the V DWR. The complete data set related to the first drying tunnel is reported as an example at fig. 3. Characteristic drying zones were delimited by green lines. The temperature and relative humidity profiles, registered in the VI DWR, are presented for all drying tunnels at fig.4a and fig.4b. The illustration of the "false" air progress for each drying tunnels is presented at fig. 4c. Measured and calculated energy and mass balances are given in tables 2 - 5. The outlet fan at the right side of the exhausted air duct 2b (position 5) was not functional during the measure. The average mass of green and dried products was respectively 11.32 and 9.07 kg. The low level of measured mass divergence was registered in the case of green products. The opposite situation was found in the case of dried products. The divergence value was even more for the products dried in different tunnels.

Table 1. List of inlet outlet and false air positions

	Inputs	Outputs	False air
1	Hot air duct at IV channel	Exhaust air duct 1a – fan at the right side	Under revision door
2	Hot air duct after IV channel	Exhaust air duct 1b – fan in the middle	From returning tunnel
3	Hot air duct after III channel	Exhaust air duct 1c – fan at the left side	From the inlet door
4	Hot air duct after II channel	Exhaust air duct 2a– fan at the right side	Around the exhausted channels
5	Hot air duct of the Heat generator	Exhaust air duct 2b – fan in the middle	
6	/	Exhaust air duct 2c – fan at the left side	

Table 2. Registered and calculated values of mass and energy on inlet positions

Inputs	Date	T (°C)	H (kg/kg)	υ (m^3/kg)	i (kJ/kg)	w (m/s)	V (m^3/h)	M (kg/h)	E (MJ/h)	ΔE (MJ/h)
1	05.04.	194	0.0045	1.3315	207.9	20.54	96148.6	72211.7	15010.0	13103.6
1	07.04.	194	0.0055	1.3336	210.7	20.88	97731.5	73283.3	15442.7	12951.0
1	12.04.	181	0.008	1.3017	204.6	20.91	97873.5	75191.0	15385.7	13062.3
2	05.04.	194	0.0045	1.3315	207.9	16.20	75796.1	56926.1	11832.7	10329.9
2	07.04.	185	0.0055	1.3079	201.6	15.93	74548.0	56997.7	11489.9	9552.0
2	12.04.	178	0.008	1.2931	201.6	15.84	74123.6	57324.1	11554.3	9783.0
3	05.04.	191	0.0045	1.3229	204.8	12.60	58966.4	44572.6	9129.4	7952.6
3	07.04.	185	0.0055	1.3079	201.6	11.66	54582.3	41732.4	8412.6	6993.7
3	12.04.	177	0.008	1.2902	200.5	11.13	52084.6	40369.5	8095.7	6848.3
4	05.04.	186	0.0045	1.3087	199.8	6.37	29808.6	22777.8	4549.9	3948.6
4	07.04.	182	0.0055	1.2993	198.5	6.65	31106.2	23940.0	4753.0	3939.0
4	12.04.	194	0.008	1.3389	217.9	6.23	29162.5	21780.4	4745.7	4072.6
5	20.04	107.5	0.041	1.1482	218.7	24.90	2814.7	2451.4	536.0	444.6

Date	M IV (kg/h)	M III (kg/h)	M II (kg/h)	M I (kg/h)	ΔE IV (MJ/h)	ΔE III (MJ/h)	ΔE II (MJ/h)	ΔE I (MJ/h)
05.04.	15285.7	12353.5	21794.9	22777.8	2773.7	2377.2	4004.1	3948.6
07.04.	16285.5	16628.2	18589.2	21780.4	3399.1	2703.7	2775.6	4072.6
12.04.	17867.0	15530.0	18980.9	22813.2	3279.4	2805.0	3249.7	3728.3
Average value	16479.4	14837.23	19788.33	22457.13	3150.733	2628.633	3343.133	3916.5

Table 3. Registered and calculated values of the "false" air breakthrough

Inputs	Date	T (°C)	RH (%)	H (kg/kg)	υ (m^3/kg)	i (kJ/kg)	w (m/s)	V (m^3/h)	M (kg/h)	E (MJ/h)	ΔE (MJ/h)
1	12.04.	18.9	55	0.0075	0.8362	38.0	4.10	22066.2	26387.4	1001.4	-1.3
2	07.04.	23	55	0.0075	0.8480	42.1	2.20	51242.4	61298.1	2320.0	2.9
3[1]	12.04	19.3	56	0.0075	0.8374	38.4	1.90	3687.9	3523.2	135.144	-2.2
4	07.04.	31	70	0.02	0.8882	82.2	1.60	21026.3	23672.0	1945.1	1379.3
Sum:	/	/	/	/	/	/	/	98022.8	114880.7	5401.644	1378.7

3[1]- Calculated for the time period when the doors are opened (4 DWW/h x 60s)

Table 4. Registered and calculated values on outlet positions

Date	08.04	11.04	12.04
Ha (kg/kg)	31.7	36.8	34.8
i_0	0.005	0.008	0.007

Outputs	T (°C)	RH (%)	H (kg/kg)	υ (m^3/kg)	i (kJ/kg)	W (m/s)	V (m^3/h)	M (kg/h)	E (MJ/h)	ΔE (MJ/h)	ΔH_2O (kg/h)

1	30,6	72	0.02	0.8871	81.8	17.50	39440.4	44461.6	3634.8	2225.4	653.8
1	28,4	86	0.021	0.8820	82.0	17.50	39440.4	44716.3	3666.8	2021.3	569.4
1	37	68	0.027	0.9157	106.4	16.83	37937.9	41432.2	4407.0	2965.1	806.9
2	28,5	80	0.0195	0.8802	78.3	18.63	41994.6	47707.9	3734.9	2112.9	655.1
2	31	77	0.022	0.8910	87.3	18.63	41994.6	47131.6	4113.2	2619.1	784.0
2	29,5	94	0.0245	0.8901	92.1	18.63	41994.6	47181.7	4344.0	2607.7	759.9
3	32,9	84	0.027	0.9036	102.0	19.98	45037.1	49844.5	5085.8	3505.7	1067.8
3	30,7	94	0.0265	0.8964	98.4	19.98	45037.1	50244.4	4945.7	3096.7	905.5
3	40,8	72	0.0355	0.9391	132.2	21.65	48793.4	51960.3	6870.4	5062.2	1430.1
4	32,9	73	0.023	0.8980	91.8	17.13	38614.0	43001.3	3948.2	2585.0	756.6
4	30,3	82	0.0225	0.8896	87.8	17.13	38614.0	43403.7	3811.4	2214.1	615.5
4	37,7	75	0.0315	0.9241	118.6	15.75	35496.3	38411.5	4557.2	3220.5	912.3
5 - 8.04	31,6	28	0.008	0.8733	52.2	-8.32	-11824	-13539	-706.4	-277.2	-40.3
5 - 1.04	28,6	42	0.0105	0.8682	55.5	-8.32	-11824	-13620	-755.6	-254.4	-33.7
6	32,9	69	0.022	0.8966	89.3	17.72	39928.7	44534.6	3975.2	2563.4	740.8
6	29,7	80	0.021	0.8858	83.4	17.72	39928.7	45075.5	3757.5	2098.7	573.9
6	33,3	44	0.014	0.8866	69.2	14.42	32491.3	36648.2	2537.5	1262.1	253.0
Sum:	/	/	/	/	/	/	/	211672	16759.9	13120.8	3791.2

Table 5. Mass and energy balances

Mass Balance	Inlet (kg/h)	Outlet (kg/h)	Energy balance	Inlet (MJ/h)	Outlet (MJ/h)
product mass	17332	13840	product mass	-	28
hot air	73562.09	-	Exhaust air from the kiln	11230	-
moisture air	-	211672.3	air from heat generator	2311	444.6
Total	90894.09	225512.3	Moisture air	-	13120.8
∑Outlet - ∑ Inlet	-	134618.2	Total	13541	13593.4
			∑Outlet - ∑ Inlet	52.4	-

The total drying cycle (not taking into account the time spent in the return channel) has lasted 45h for the products dried in tunnel I. The Bigot curve (figure 3l) indicates that the raw material composite is sensitive to drying. The weight loss in the critical point was 8.5%. This point was reached after 12h in the V DWR at the 7th DWW position. The critical point in the II and X DVR was achieved respectively at the 11th and 19th DWW position after 19 and 35h (see figure 3g or figure 3h.).This means that the available quantities of "useful" drying air were insufficient. The air distribution within the drying tunnel was uneven (see figure 3a – 3d.). The “false” air has at least breakthrough into the drying space area of the last 5 DWW. The most pronounced oscillations of the drying air temperatures were registered in the II DWR which means that the lower DWW part is mostly affected by the "false" air. The warmer air rises towards the upper DWR, providing the shortest drying time in the middle of the DWW. It was registered that one of the 13 air mixers was not working properly for 7h. This time period is clearly detonated by two vertical lines at figure 3a.

Since the hot air mass-flow rate with dry base, heat transfer coefficient, specific heat of wet air for the water–air system, the surface area of drying ware per unit length of dryer, saturated, critical and final humidity were known it was possible to calculate the theoretical length of the constant drying zone inside the drying channel. This value was estimated at 20,5m. If Zc is expressed in DWR units it is equal to 9th DWR position. From this point out the drying process can be accelerated without the fear of the product cracking. It can be seen that the theoretical Zc value is nearly the same as the corresponding critical point reached in the middle part of the DWW. The opposite situation was registered when the critical point determined in upper or lower DWRs was compared with the theoretical one. This means that the drying profile registered in V DRW is very close to the ideal one. The residual moisture of the dried products taken from the DWW middle part was in the vicinity of the desired one. That was not the case for the products taken from the lower or upper DWRs. The desired residual moisture in those products was overreached. In other words some products are "wet" while some are dried more than it is necessary. The uneven quality and the presence of "wet" products was the reason of increased cracking scarp rate at the beginning of the firing process.

Since the dryer works under the pressure large quantities of the "false" air are transported into the dry space, which significantly limits the ability to control the drying regime. The advantages of the established drying regimes in the first two drying tunnels in relation to the third and fourth can be clearly seen of figure 4. The calculated "false" air progress along the drying tunnels was also reported. It can be seen that tunnel IV is the mostly affected by the "false" air. This is expected result since the tunnels which are closer to the returning dryer channel are predisposed to receive larger amounts of the "false" air. The mass balance difference reported in table 5 corresponds to the total quantity of the "false" air breakthrough. The identified "false" air quantities reported in table 3 are 15% lower than the one given in table 5. The fan at the right side of the exhaust air duct 1a ("false" air position 1) was working 50 percent slower during the second measuring day (results from 12.04). In other words all relevant "false" air sources were properly identified and quantified. For evaporation of the 3791 kg of water 13593.4 MJ/h is used. This means that the energy used to evaporate 1kg of water is 3,585 MJ/h. This is a very good result. For example the specific energy consumption of the much modern Zeypr dryer driers is 3250 MJ/h (from the Cleia webcite).

3a

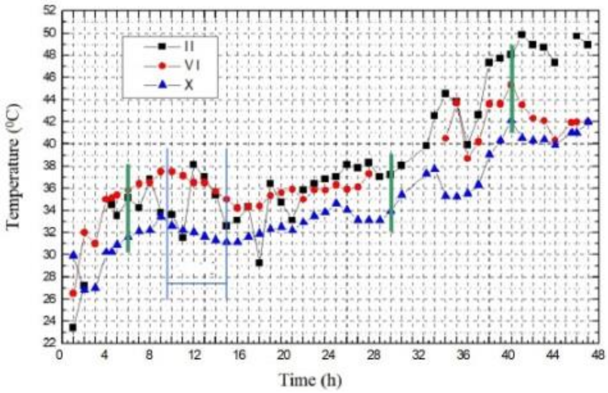

3b

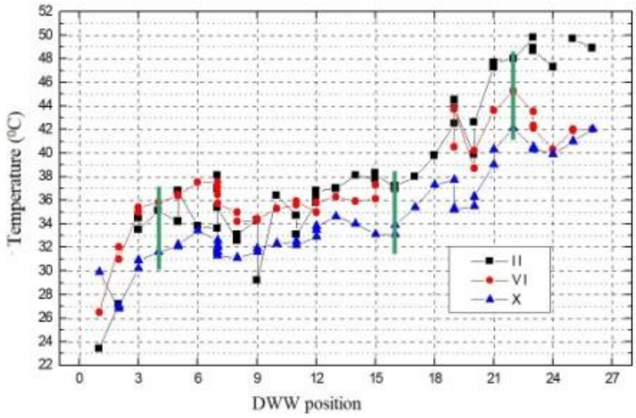

3c

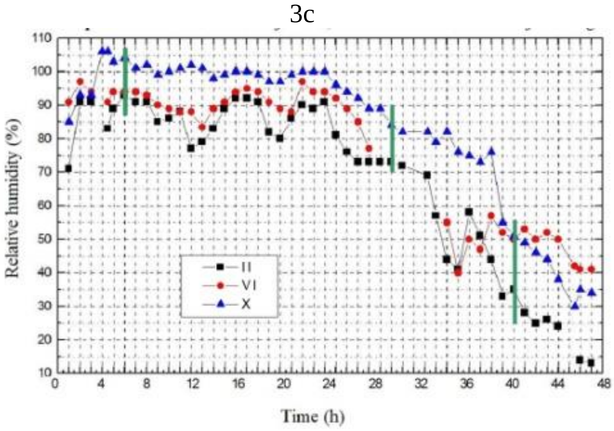

3d

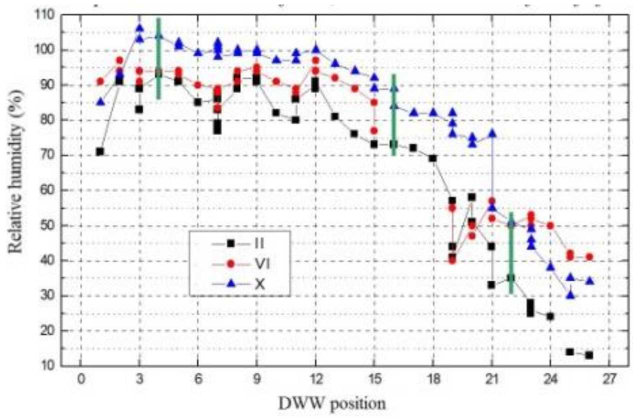

3e

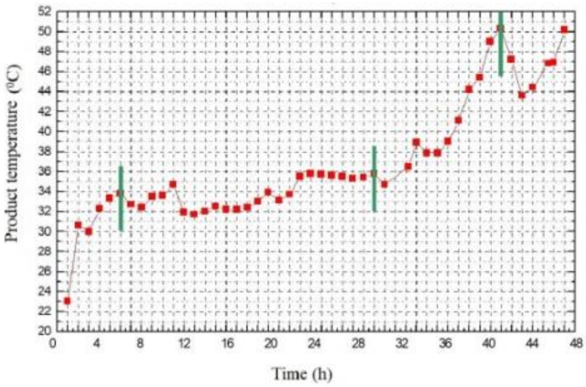

3f

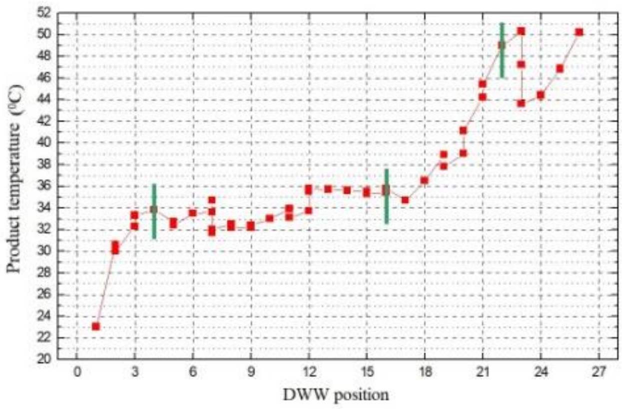

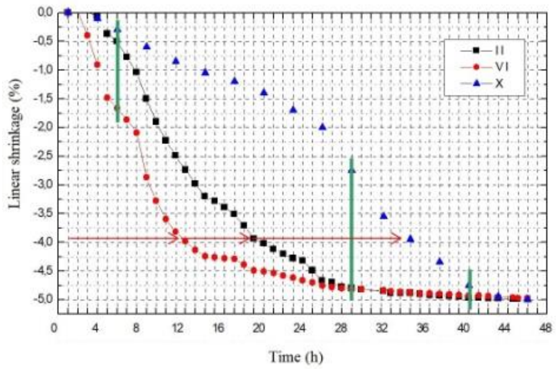

3g

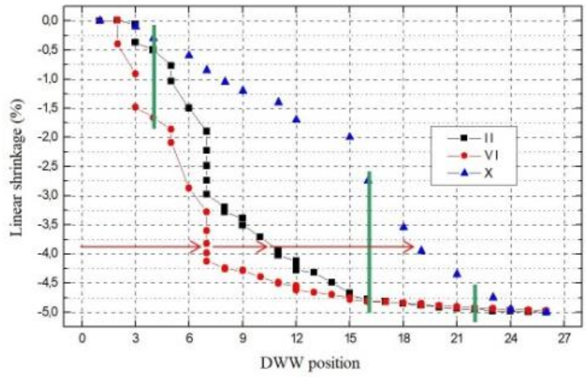

3h

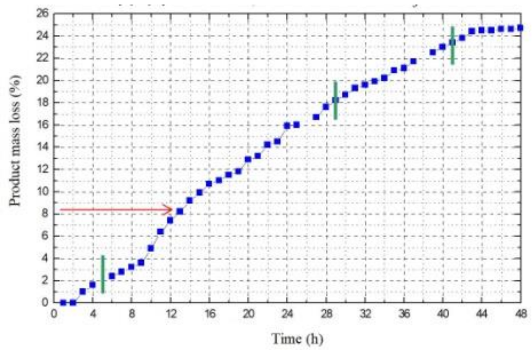

3i

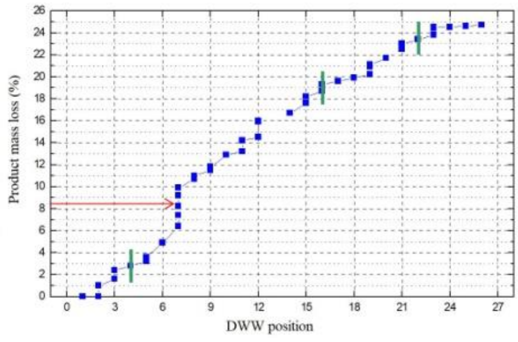

3j

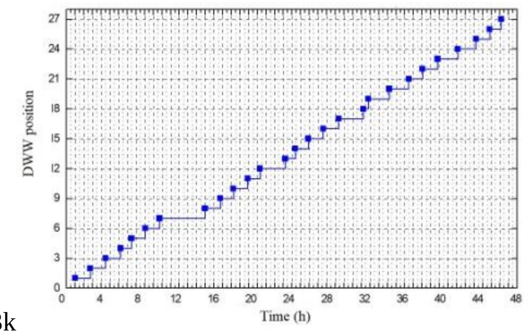

3k

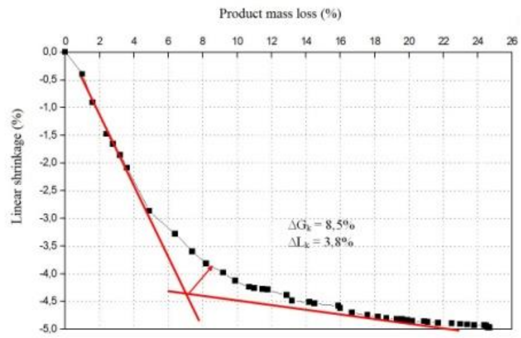

3l

Fig. 3. Registered drying data in the tunnel 1

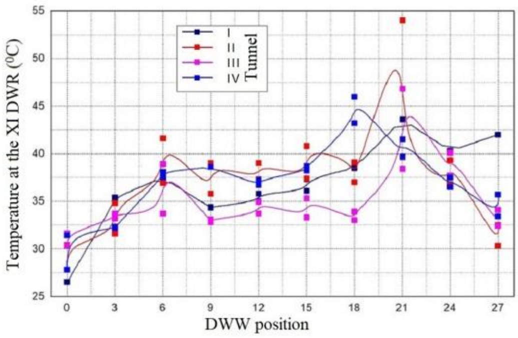

4a

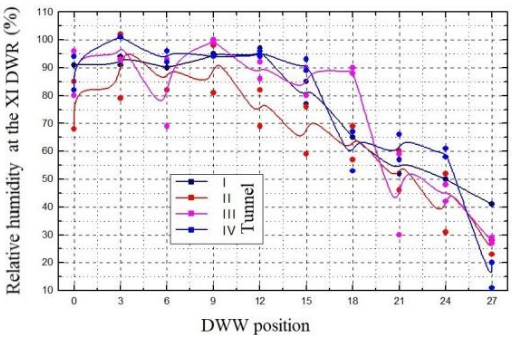

4b

Schematic view of the "false" air breakthrough

4c

Fig. 4. Registered temperature and humidity profiles in the middle of the drying tunnels

Based on the factory management expectation to raze the production to the level of 50,000 hollow blocks, presented mass and balance results and registered drying regime, the project solution related to the drying process upgrade was created. Four starting assumptions were specified. The forming process is organized in three daily shifts. Total drying time is 43h. The raw material composite is not changed as well as the green product moisture content. The firing process is organized in two kilns. Technical information related to the proposed drying process upgrade is given in table 6. It is interesting that the reduction of the moisture content in the green ware by only 1% will consequently lower the total net energy potential by almost 4%. The existing dryer hot air fan capacity of 74000 kg/h is lower than the specified hot air volume value. In other words it is necessary to provide additional two fans. The current quantities of hot air from the kiln and the heat generator are also not adequate for the specified production upgrade. That was the reason why one of the starting assumptions was to use two kilns. In order to achieve the desired production capacity and to keep the energy efficient production the proposal was that each kiln works with the 70% of its maximal capacity. The capacity of the existing moisture air fans is adequate.

Table 6. Technical data of the proposed upgrade

1	The forming block capacity – (block/min)	33
2	The DWW has to be pulled into the drying tunnel every - (min)	12
3	The daily pulling rate – (DWW/day)	33
4	The daily block production – (blocks/day)	47520
5	The quantity of water vapor evacuated from the dying space - ΔH_2O (kg/h)	4630
6	The minimal quantity of drying air - M (kg/h)	186000
7	Minimal net energy potential - E (MJ/h)	17950
8	Hot air temperature (^0C)	107
9	Hot air volume flow - V (m^3/h)	202000
10	Current situation - capacity of the existing fan (m^3/h)	74000
11	Capacity of the additional hot air fan (m^3/h)	93000
12	Current situation - registered hot air from the exhaust kiln air (kg/h)	40000
13	Current situation - registered hot air from the heat generator (kg/h)	34000
14	Net energy of the exhaust air from kiln 1 and 2 - (MJ/h)	15722
15	Net enery taken from the kiln 1 and 2 mantle - (MJ/h)	1230
16	Net energy of the heat generator 1 and 2 - (MJ/h)	1870
17	Moisture air flow – V (m^3/h)	192000

The moisture air flow inside the drying tunnel should achieve an absolute humidity of 31g water vapour/kg dry air (25g is from the product). In other words the outlet air has 80% relative humidity and is at 36^0C.

4. CONCLUSION

The Keller classical countercurrent dryer was monitored for a month. The drying regimes were recorded in each drying channels. The uneven distribution of the drying air within the drying tunnel was registered. The fact that dryer works under with the pressure drop was confirmed. The relevant "false" air sources were properly identified and quantified. The lower DWR were mostly affected by the "false" air. The shortest drying time was registered in the central part of the DWW. The residual moisture of the dried products was irregular along the height of the DWW. Some products were "wet" while some were dried more than it is necessary. The increased firing scarp rate was connected with the presence of "wet" products in the kiln. The theoretical length of the constant drying zone inside the drying channel was determined and compared with the critical length determined for the products in the upper middle and lower DWRs. It was confirmed that the drying profile registered in the middle DRW was close to the ideal one. The upgrade of the existing drying line was specified in detail. The reported solution was based on the reported material and energy balances and the factory management decision to raze the production to the level of 50,000 hollow blocks.

Acknowledgement: This paper was financed by ministry of education science and technological development of Serbia, contract number 4451-03-68/2022-14/ 200012. Authors: M. R. Vasić is fully employed in the Institute for testing of Materials

5. REFERENCES

1. Communication from the commission to the European parliament and the council, (2012). *Strategy for the sustainable competitiveness of the construction sector and its enterprises*, Brussel, 31.7.2012, COM (2012) 433 final.
2. Communication from the commission to the European parliament and the council the European economic and social committee and the committee and the committee of the regions (2012). *A resource-*

efficient Europe – Flagship initiative under the Europe 2020 Strategy, Brussel, 26.1.2011, COM (2012) 21 final.
3. Shokouhmand H, Abdollahi V, Hosseini S, Vahidkahah K, (2011). *Performance optimization of a brick dryer using porous simulation approach*, Drying Technology 29 3 pp 360-370.
4. Dolanc. G, Vladimir. J, (1997). *Improvement of the drying process control in a clay product plant*, IAF Proceeding 30 6 pp. 1575-1580.
5. Velthuis M.F.J, Denissen M.A.J, (1997). *Simulation model for industrial dryers: reduction of drying times of ceramics &saving energy*, Drying Technology 15 6-8 pp 1941-1948.
6. Telljohann U, Junge K, (2008). *Moisture diffusion coefficients for modeling the first and second drying section of green bricks*, Drying Technology 26(7), 855-863.
7. Mancuhan E. (2009). *Analysis and optimization of drying of green brick in a tunnel dryer*, Drying Technology 27(5), 707-713.
8. Vasić M, Grbavčić Ž and Radojević Z (2014). *Analysis of Moisture Transfer During the Drying of Clay Tiles with Particular Reference to an Estimation of the Time-Dependent Effective Diffusivity,* Drying Technology 32(**7),** 829-840
9. Vasić M, Rekecki R, Radojević Z (2018). *A procedure for setting up the drying regime that is consistent with the nature and properties of clay raw material*, Drying Technology 36(**3),** 267-282.

Received: May 22, 2022 / Accepted: December 15, 2022 / Paper available online: December 20, 2022